Fig. S1. Rose diagrams showing large membrane protrusion directionality around the cell circumference. Diagrams depicting the circular frequency and distribution of ectodermal cell large protrusions are shown for each experimental condition: wild type, *vangl2*$^{m209/m209}$ mutant embryos, *glypican4*$^{m119/m119}$ mutant embryos, *vangl2* mRNA injected wild-type embryos, *prickle1a* morpholino (MO) injected wild-type embryos, *fn1a/1b* MO injected embryos, and *fn1a/1b* mRNA injected *vangl2*$^{m209/m209}$ mutant embryos. The horizontal plane represents 0° and a mediolateral protrusion orientation while the vertical plane represents 90° and a anterior-posterior protrusion orientation. The position of the dorsal embryonic axis is indicated.

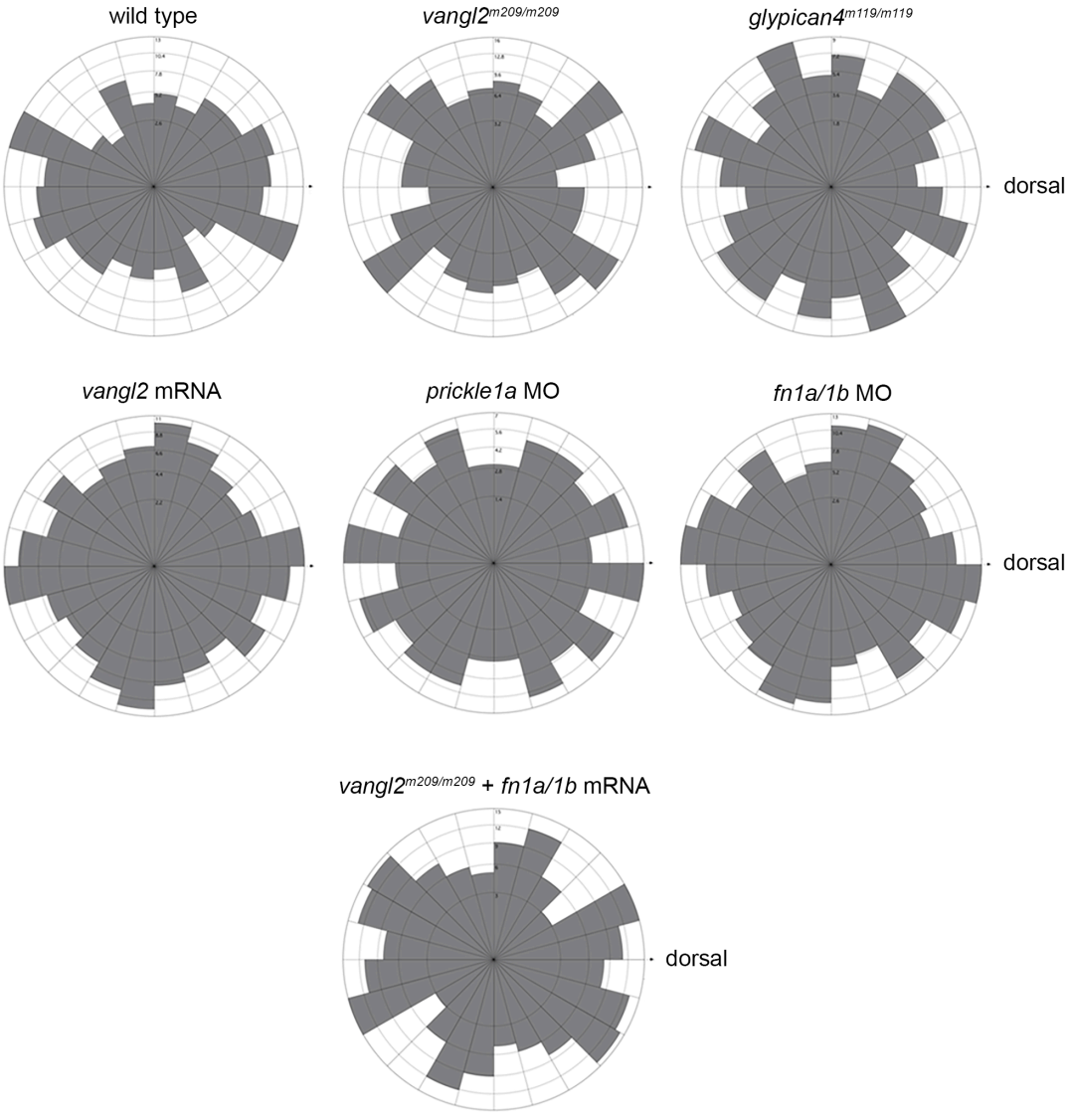

Fig. S2. Zebrafish Vangl2 polyclonal antibody validation and Vangl2 overexpression. (A) Immunofluorescence labeling of endogenous Vangl2 protein expression in wild-type (WT) tailbud stage embryo (right panel, nuclei labeled with DAPI). (B) Vangl2 expression in a wild-type embryo injected with 200 pg synthetic *vangl2* mRNA (right panel, nuclei labeled with DAPI). (C) Endogenous Vangl2 expression in a tailbud stage *vangl2*$^{vu7/vu7}$ mutant embryo. Only background fluorescence from the secondary antibody is visible. Scale bars: 5 μm in panels A and B; 20 μm panel C.

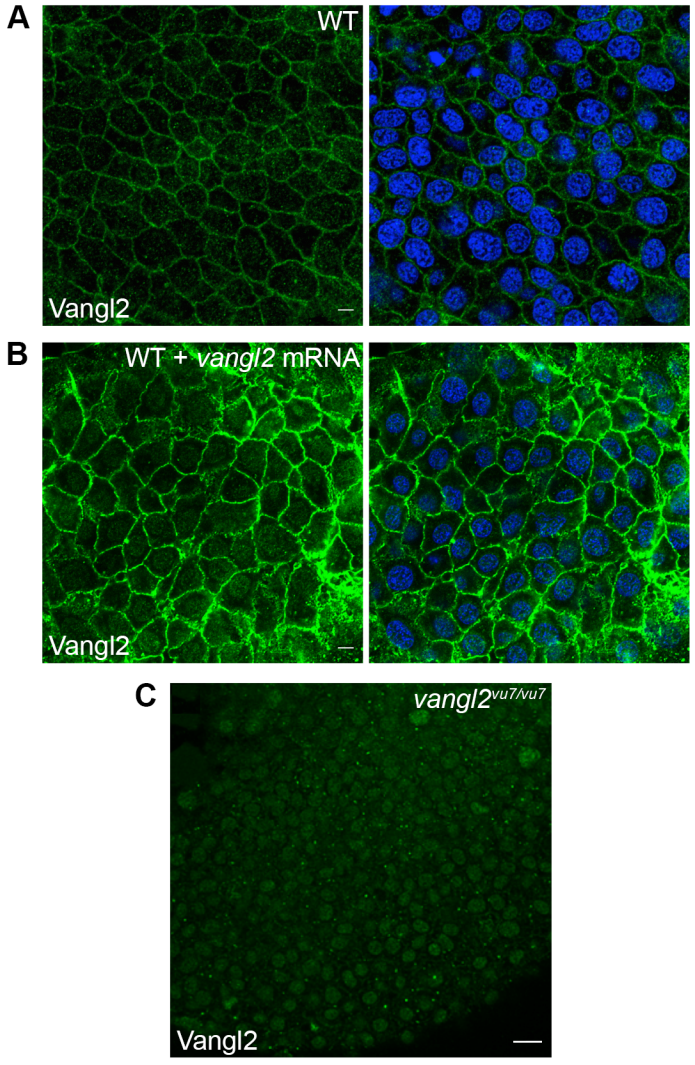

Fig. S3. Vangl2 overexpression disrupts PCP and membrane protrusion dynamics. (A) Western blot of Vangl2 protein expression in *vangl2* mRNA-injected wild-type (WT) embryos. Raw unmodified densitometry values are shown. (B) Upper panels, live images of late yolk-plug closure/tailbud stage embryos. Black lines denote the polster-tailbud angle. Lower panels, whole-mount *in situ* hybridizations performed using antisense RNA probes labeling the neural/non-neural ectoderm boundary (*dlx3b*), midline (*shha*), and prechordal mesendoderm (*ctslb*). (C) PCP and migration velocity quantitation in the ectoderm. LWR and MLA values were obtained from: wild type n values are as in Fig. 2; *vangl2*-injected wild type n=50 cells, 9 embryos. (D) Representative ectodermal cell expressing memGFP over three time points from time-lapse data. (E,F) Quantitation of the average total number of protrusions and the total percentage of polarized protrusions in wild type (n values are as in Figs 2 and 3) and *vangl2*-injected wild-type embryos (n=10 cells, 7 embryos). (G) Directed migration values (wild type n values are as in Fig. 3; *vangl2*-injected n=43 cells, 9 embryos). (H) Schematic representations of the migration paths of individual ectodermal cells. Origins (arrows) standardized for comparison. Dorsal is to the right. Average values are shown ± standard deviation. $^{**}P<0.01$, $^{****}P<0.0001$; *P* values are versus wild type; two-tailed unpaired *t*-test. Scale bar, 5 μm.

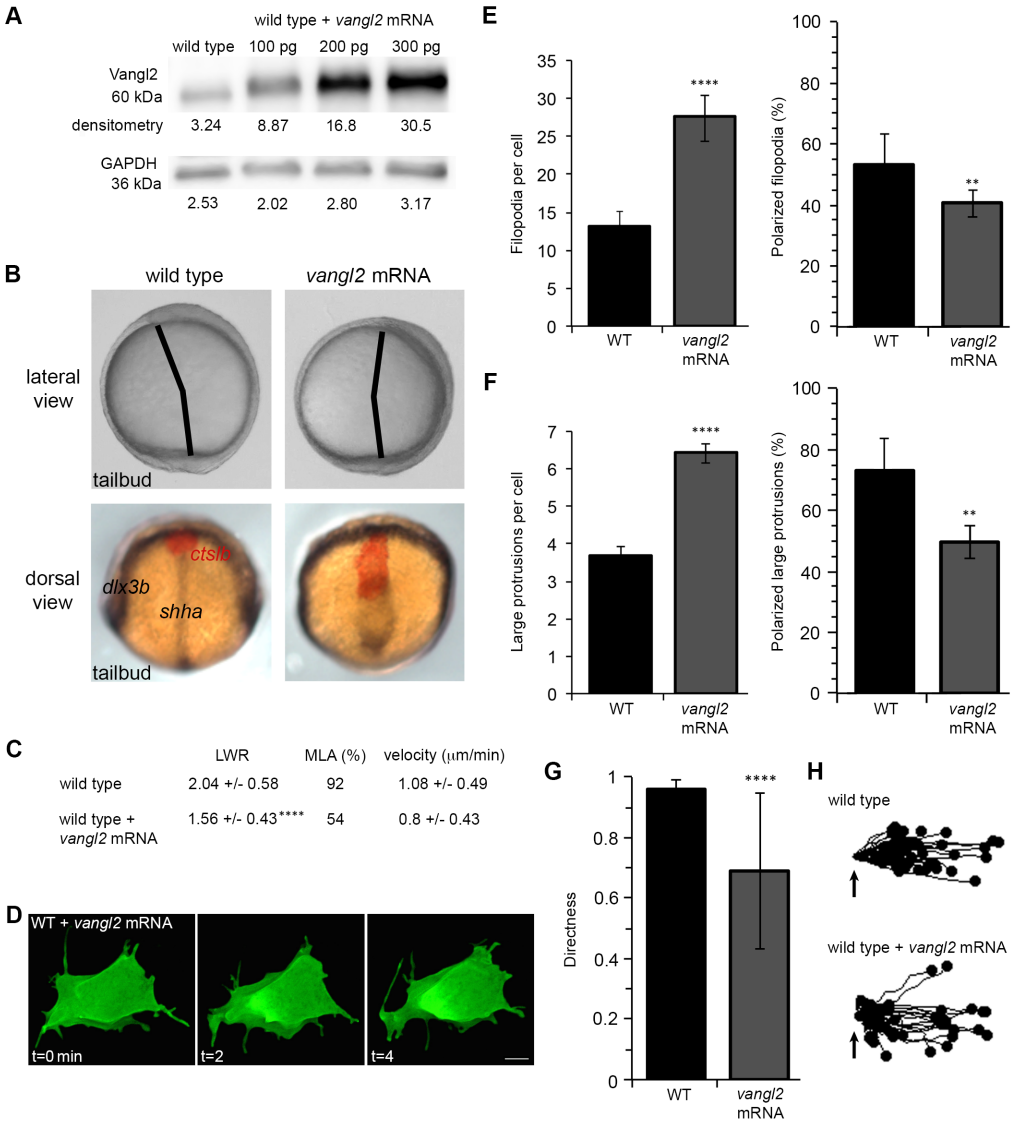

Figure S3

Fig. S4. Vangl2 expression in polarized migrating gastrula cells. (A) Tailbud-1-somite stage wild-type lateral ectodermal cells injected with memRFP and GFP-VANGL2 synthetic mRNA. (B,D) Plot profiles of fluorescence intensity (F.I.) across the anterior/posterior (B) and leading edge/trailing edge (D) axes of single ectodermal cells. (C,E) memRFP and GFP-VANGL2 anterior/posterior (C) and leading edge/trailing edge (E) membrane F.I. ratios for individual lateral ectodermal cells (anterior/posterior n=18 cells, 15 embryos; leading edge/trailing edge n=20 cells, 15 embryos). Horizontal and vertical red and green lines indicate averages. n.s. not significant; two-tailed paired *t*-test. Scale bars, 5 μm.

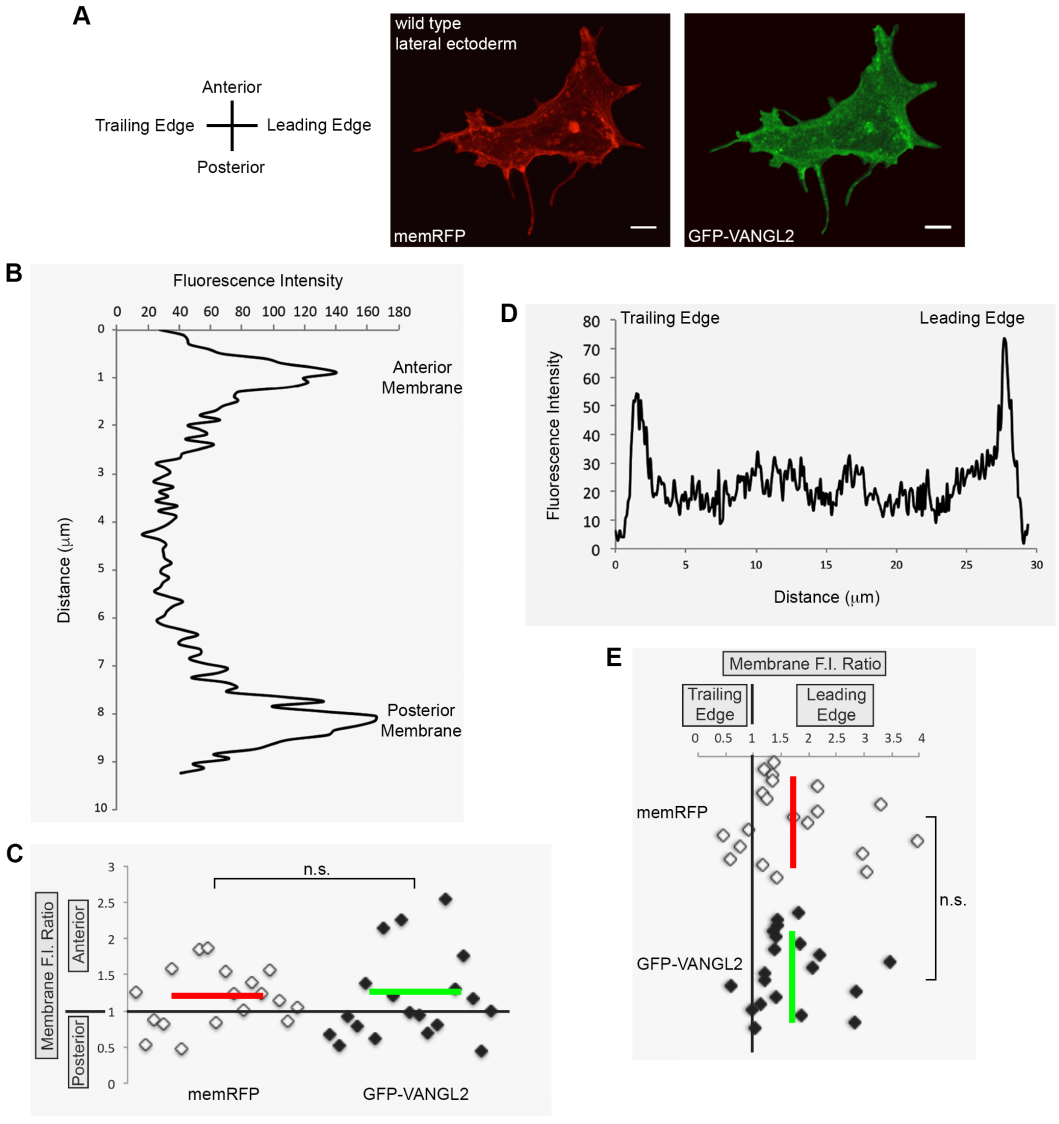

Fig. S5. GFP-VANGL2 localization in protrusive and non-protrusive membrane domains. (A) Lateral ectodermal cell labeled with memRFP and GFP-VANGL2. Arrows denote a forming non-polarized large protrusion. Arrowheads show a non-protrusive membrane domain. memRFP and GFP-VANGL2 fluorescence intensity (F.I.) ratios for (B) protrusive/non-protrusive membrane domains (n=9 protrusions, 6 embryos) and (C) polarized/non-polarized large protrusions (n=14 protrusions, 5 embryos). Vertical red and green lines indicate the averages. *P<0.05, n.s. not significant; two-tailed paired t-test. Scale bars, 5 μm.

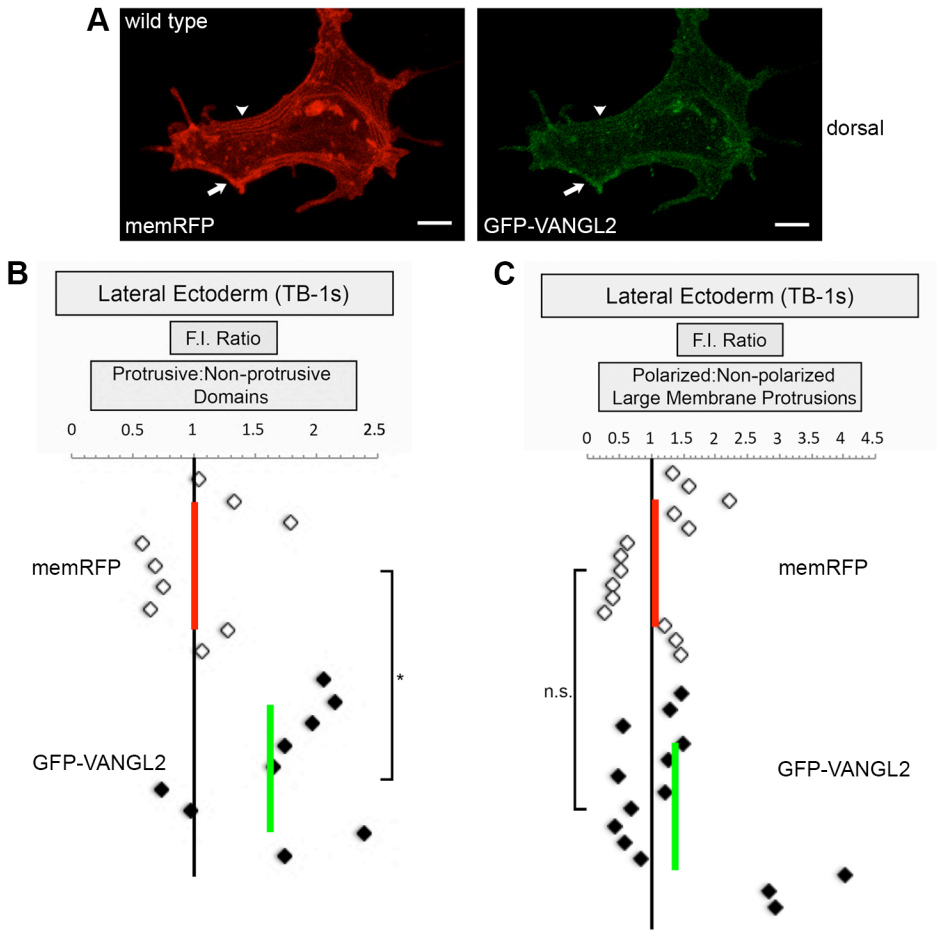

Fig. S6. Morpholino knockdown disrupts fibronectin expression and fibrillogenesis. (A) Immunofluorescence labeling of fibronectin expression in tailbud stage wild-type embryo and wild-type embryos injected with either 5 ng or 10 ng of each *fibronectin* morpholino (MO). (B) Injection of *fn1a/1b* synthetic mRNA rescues the *fn1a/1b* morpholino ECM phenotype. Bottom images in (A) and (B) show DAPI-labeled nuclei. Scale bars, 5 µm.

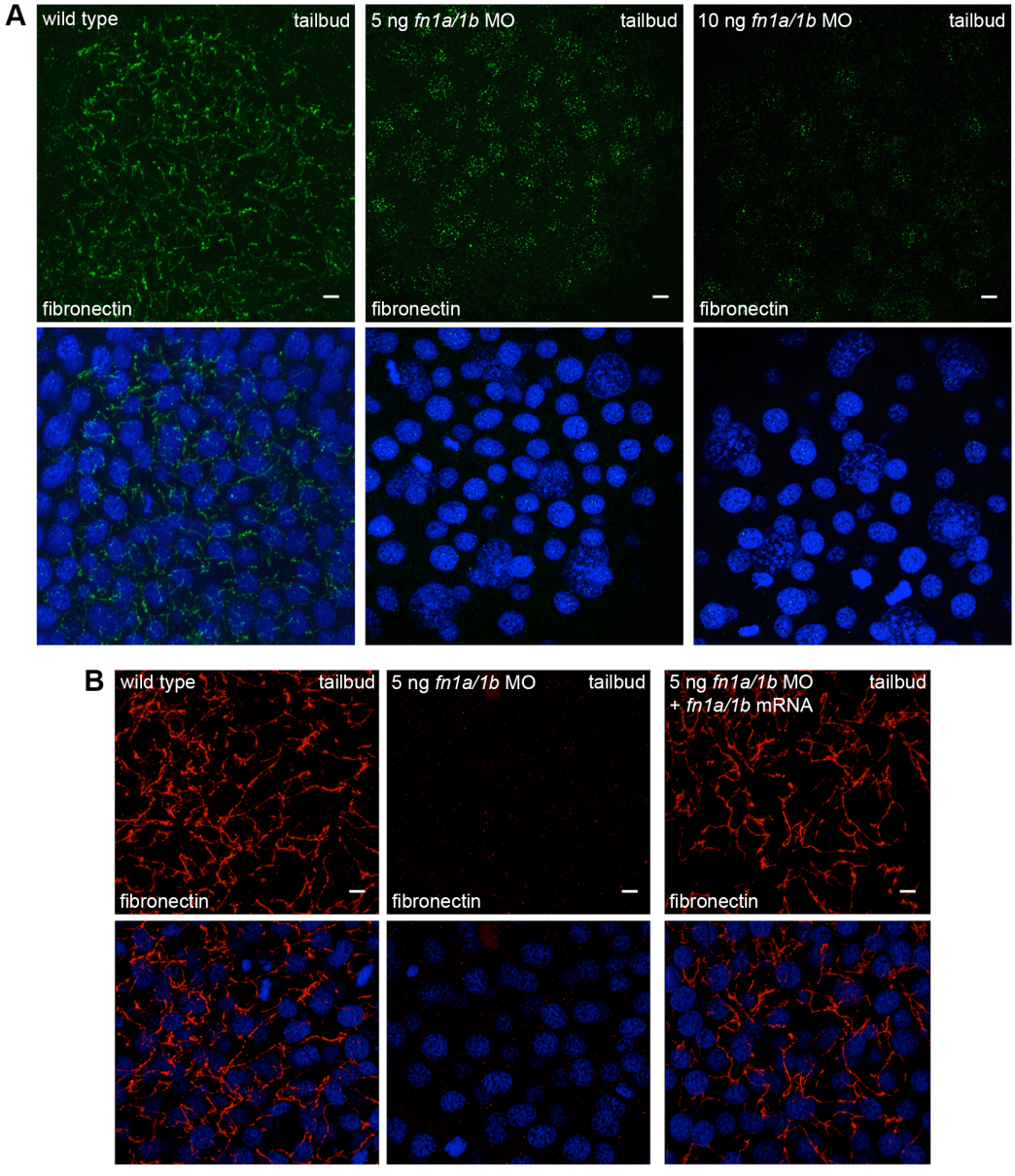

Fig. S7. Wild type and *vangl2* morphant membrane protrusive activity at mid-gastrulation. (A) Time-lapse confocal images of 80% epiboly epiblast cells expressing memGFP. WT, wild type. (B,C) Quantitation of the total numbers of membrane protrusions formed by wild type (n=9 cells, 7 embryos) and wild-type embryos injected with *vangl2* morpholino (MO) (n=10 cells, 6 embryos). (D) Quantitation of the total percentage of polarized large protrusions. Average values are shown ± standard deviation. ***P*<0.01; *P* values are versus wild type; two-tailed unpaired *t*-test. Scale bars, 5 µm.

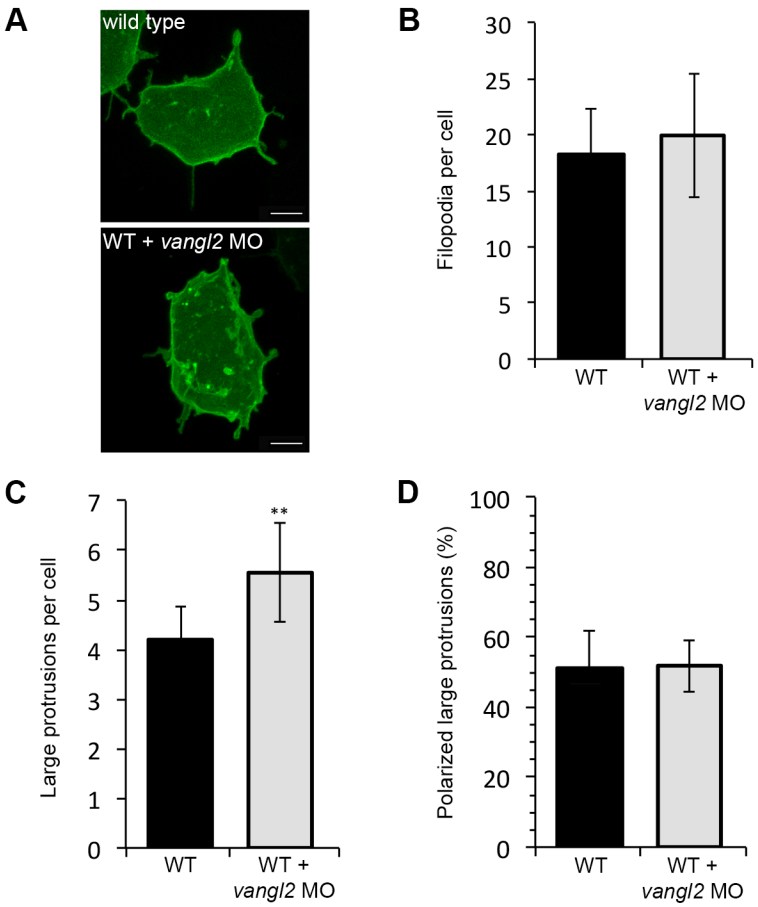

Fig. S8. Fibronectin is not required for Vangl2 expression at 60% epiboly. (A) Immunofluorescence labeling of Vangl2 protein expression in wild type and *fn1a/1b* morpholino (MO)-injected wild-type embryos without (left panels) and with (right panels) DAPI nuclear labeling. (B) Representative plot profiles showing the average fluorescence intensities across single epiblast cells in wild type (n=30 cells, 3 embryos) and *fn1a/1b* morphant embryos (n=30 cells, 3 embryos). Scale bars, 5 μm.

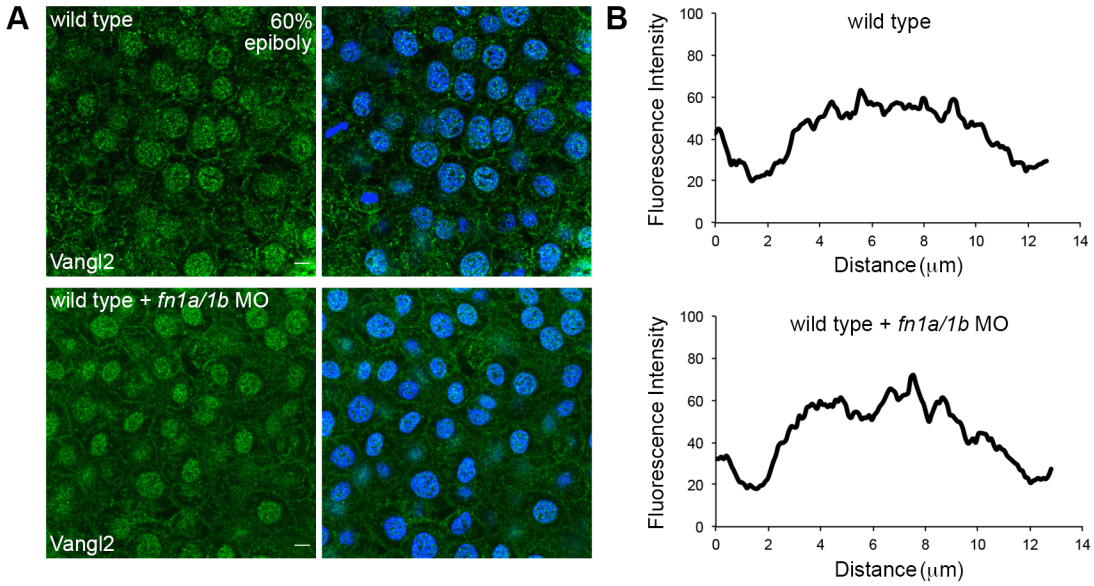

Fig. S9. Western blot analysis of Vangl2 expression in *fibronectin* morphants. Blots of total protein extracts from wild-type control embryos and wild-type embryos injected with 3, 6, 5, and 10 ng of each *fibronectin* morpholino (MO). Vangl2 labeled with a rabbit polyclonal antibody and actin loading control. Densitometry numbers for Vangl2 are normalized to actin.

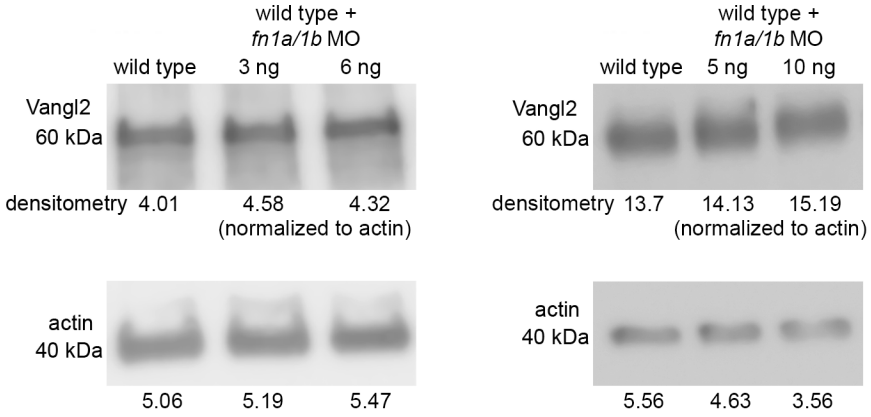

Fig. S10. Knockdown of fibronectin in *vangl2* mutant embryos. (A) Time-lapse confocal image of late gastrula stage cell expressing memGFP. *vangl2* mutant embryo injected with *fn1a/1b* morpholinos (MO). (B,C) Quantitation of the total numbers of membrane protrusions formed by *vangl2* mutant embryos injected with *fn1a/1b* MO (n=5 cells, 3 embryos). The data from wild type (WT), *vangl2* mutant embryos, and wild-type embryos injected with *fn1a/1b* MO are shown for comparison. (D) Quantitation of the total percentage of polarized large protrusions. Average values are shown ± standard deviation. ****P<0.0001; P values are versus wild type; one-way ANOVA significance test followed by Tukey HSD post-hoc tests. Scale bar, 5 μm.

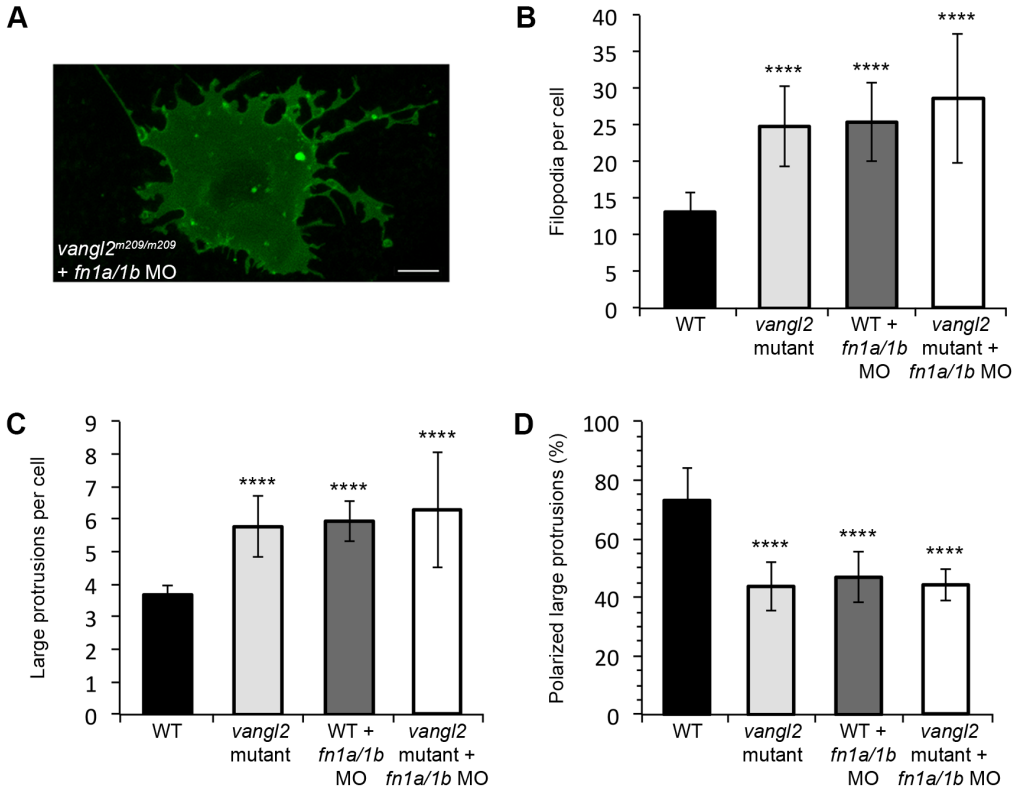

Fig. S11. *vangl2* mRNA overexpression in *fn1a/1b* morphant wild-type embryos. (A) Time-lapse confocal image of late gastrula cell expressing memGFP. *fn1a/1b* morpholino (MO) injected wild-type embryo co-injected with synthetic *vangl2* mRNA. (B,C) Quantitation of the total numbers of membrane protrusions formed by wild-type embryos injected with *fn1a/1b* MO and *vangl2* mRNA (n=5 cells, 4 embryos). The data from wild type (WT), *vangl2* mRNA injected wild-type embryos, and *fn1a/1b* MO injected wild-type embryos are shown for comparison. (D) Quantitation of the total percentage of polarized large protrusions. Average values are shown ± standard deviation. ***P*<0.01, ****P*<0.001, *****P*<0.0001; *P* values are versus wild type; one-way ANOVA significance test followed by Tukey HSD post-hoc tests. Scale bar, 5 µm.

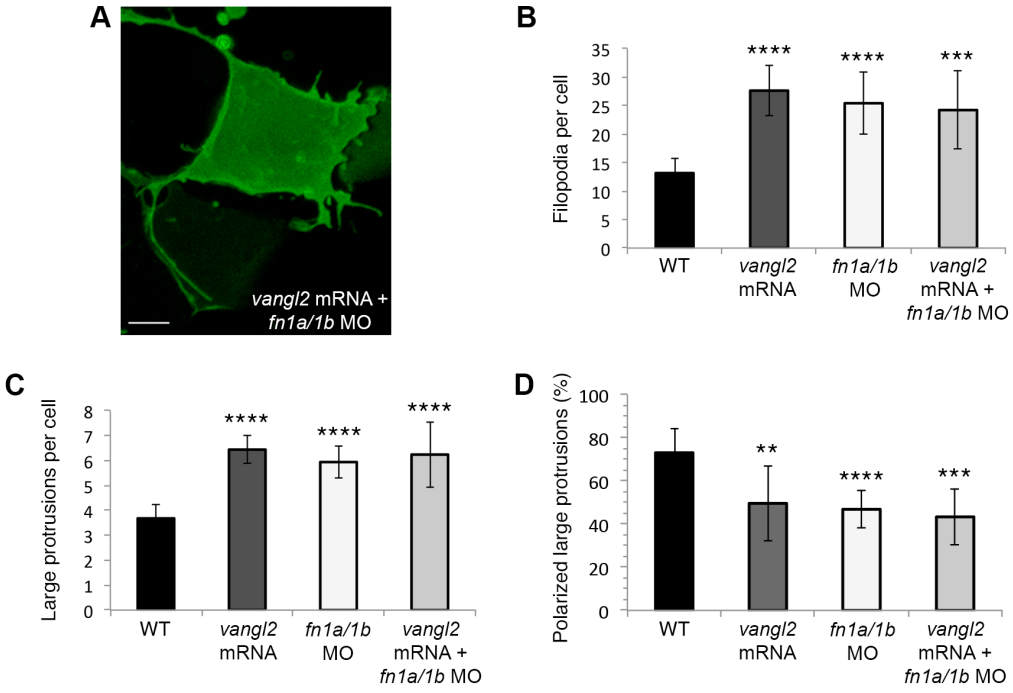

Fig. S12. Injection of *fn1a/1b* mRNA fails to rescue the *vangl2* mutant embryo convergence and extension phenotype. (A) Lateral view of a wild-type embryo at the yolk-plug closure (YPC)-tailbud stage. Black lines denote the polster-tailbud angle. (B) Lateral views of three *vangl2*$^{m209/m209}$ embryos highlighting subtle variations in the mutant convergence and extension phenotype. (C) Lateral views of three *vangl2*$^{m209/m209}$ embryos injected with *fn1a/1b* mRNA (n=50 mRNA injected homozygous mutant embryos analyzed).

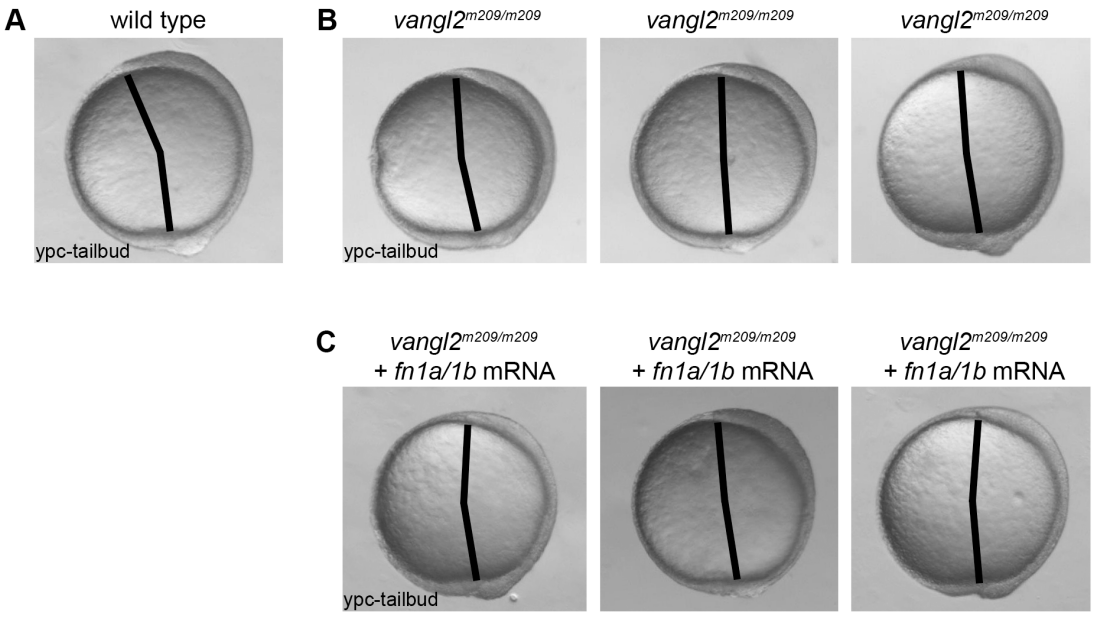

Table S1. Accumulated and Euclidean ectodermal cell translocation distances.

	Accumulated distance (μm)	Euclidean distance (μm)
wild type	19.49 +/- 8.82	18.81 +/- 8.78
vangl2$^{m209/m209}$	17.68 +/- 9.70	15.76 +/- 10.54
glypican4$^{m119/m119}$	21.22 +/- 5.05	20.02 +/- 5.18
wild type + *vangl2* mRNA	14.36 +/- 7.75	11.45 +/- 9.06
wild type + *prickle1a* morpholino	17.74 +/- 6.18	15.68 +/- 8.04
wild type + *fn1a/1b* morpholino	24.78 +/- 11.49	22.88 +/- 11.26
vangl2$^{m209/m209}$ + *fn1a/1b* mRNA	23.45 +/- 6.34	22.03 +/- 6.15